Journal of Engineering Mathematics (2005) 51: 1–13

Non-Newtonian effects on lubricant thin film flows

RONG ZHANG and XIN KAI LI[1,*]
Department of Computing Science, and Information Propagation, School of Sciences, Southern Yangtze University, Jiangsu, China; [1]*Faculty of Computing Science and Engineering, De Montfort University, Leicester, England;* [*]*Corresponding author: e-mail: xkl@dmu.ac.uk*

Received 25 September 2002; accepted in revised form 9 July 2004

Abstract. An analysis of non-Newtonian effects on lubrication flows is presented based on the upper-convected Maxwell constitutive equation, which is the simplest viscoelastic model having a constant viscosity and relaxation time. By employing characteristic lubricant relaxation times in all order of magnitude analysis, a perturbation method is developed to analyze the flow of a non-Newtonian lubricant between two surfaces. The effect of viscoelasticity on the lubricant velocity and pressure fields is examined, and the influence of minimum film thickness on lubrication characteristics is investigated. Numerical simulations show a significant enhancement in the pressure field when the minimum film thickness is sufficiently small. This mechanism suggests that viscoelasticity does indeed produce a beneficial effect on lubrication performance, which is consistent with experimental observations.

Key words: lubrication, non-Newtonian fluid, perturbation method, thin-film viscoelacity

1. Introduction

A fascinating and largely-unresolved problem in tribology concerns the effect of viscoelasticity on lubrication-flow characteristics. This problem has been tackled since the mid-1950s with the appearance of the so-called multigrade oils [1, pp. 111–114], [2, Chapter 1], [3, Chapter 3], [4, Chapter 6], and has recently taken on added significance with the transition to lubricants of yet lower viscosity for improved energy efficiency [5, 6]. Any factor influencing load capacity and wear in journal bearings is clearly of renewed importance; consequently, there are good practical reasons to reopen the general question of viscoelastic effects on lubrication.

Since the mid 1950s, the addition of polymers to mineral oils has become a well established practice. These additives cause the resulting lubricants to become non-Newtonian and viscoelastic [4, pp. 292–334] , [7]. Even in the simplest flow situation, it is necessary to consider more than the usual shear-stress component; indeed, the mechanical behaviour of these lubricants is potentially far more complicated than that of mineral-oil-based lubricants, which may be regarded as Newtonian fluids. It is known that polymeric-additive-containing lubricants possess a characteristic relaxation time, λ, which is the ratio of the viscosity to the elastic modulus. For lubricating oils, the fluid relaxation times might be expected to vary from 10^{-3} s to 10^{-6} s [1, pp. 50–53], [7, 8]. If a lubrication process time is of the same order, one could expect strong time-dependent effects. The Deborah number $\mathrm{De} = \lambda/T$ can be used to

measure such time dependence, where T is a characteristic time of the flow process under consideration [4, pp. 226–227], [8].

Attempts to interpret this time-dependent effect on the basis of a shear-dependent viscosity, or based on the different heat-transfer characteristics of polymeric lubricants, have proved largely unproductive, and the viscoelastic behaviour of the lubricants has been proposed as the most likely cause for the improvements in performance (see, for example, [4, Chapter 6], [7], [9, Chapter 10]). Despite popular belief and some experimental evidence with real lubricants [7], it appears that unequal normal stresses and memory effects may be relatively insignificant in automotive journal hearings [4, Chapter 6]. As a consequence, one might superficially expect that, at high shear rates encountered in well-designed optimally loaded hearings, the behaviour of multi-grade oils may not be greatly different from that of the low-viscosity base stock used to formulate oils [3, Chapter 3]. In a recent study, however, values of the minimum oil-film thickness obtained from direct measurements in an instrumented front-main bearing of an operating engine were found to correlate not with the high-temperature, high-shear-rate viscosity alone, but with a combination of the high-temperature, high-shear-rate viscosity and relaxation time (viscoelasticity). Relaxation times were calculated based on primary normal-stress measurements made using a Lodge stress-meter [6]. Even though typical fluid relaxation times are only of the order of microseconds, viscoelasticity can have a measurable and beneficial effect on lubrication characteristics [6], and is expected to significantly affect the minimum oil-film thickness and the coefficients of friction in the journal bearings [6, 10].

There is some controversy as to whether viscoelastic behaviour, as manifested through normal stress effects, can have any effect at all in lubrication, over and above that which arises as a result of the shear dependence of the viscosity [11]. It seems clear at present that polymeric oils are in fact better lubricants than the non-polymeric oils, at least in journal bearings [6, 7]. Specifically, they appear to reduce friction and hearing wear when compared with either their base oils or mineral oils of comparable low-shear viscosity. To date, attempts to predict this improvement in performance by invoking non-Newtonian behaviour have been singularly unsuccessful. It is unlikely that one could have known *a priori* whether viscoelasticity would give rise to any beneficial or adverse side effects, although the fact that one of nature's lubricants, synovial fluid, is an elastic liquid may have been a useful pointer [6, 7, 12]. Over the past decades, numerous theoretical and experimental studies have been undertaken to determine whether polymer-improved oils are more efficient than their Newtonian counterparts, even after the improved viscosity-temperature response has been accommodated [7]. It is fair to say that the situation is inconclusive and somewhat confused. At best, there have been small improvements, (see [6, 7, 9]); at worst, any effects have been within the experimental error (see [10, 11, 13]).

Early studies on thin-film flows have used lubrication theory to derive a coupled system of equations governing the spatial and temporal evolution of the film thickness [3, Chapter 3], [4, Chapter 6]. The majority of this work has concentrated on Newtonian fluids for the purpose of elucidating the fundamental mechanism of thin-film flows in various applications. Reviews of these works can be found in the books of Tanner [4, pp. 286–441], and Szeri [9, pp. 352–387]. Recently, much attention has been devoted to non-Newtonian fluids in thin film flows, since in many practical applications thin films generally exhibit non-Newtonian behaviour, as described by Dowson *et al.* [14, Chapter 3], Khayat [15], Tichy [16], Zhang [17] and in references cited therein. The aim of this article is to investigate how the presence of viscoelasticity in the lubricant thin films modifies the flow characteristics.

The lubricant behaviour will be modelled by the upper-convected Maxwell constitutive equation, which is the simplest viscoelastic model having a constant viscosity and a constant relaxation time. By employing characteristic lubricant relaxation times in an order-of-magnitude analysis, we develop a perturbation method to analyze the flow of Maxwell lubricants between two narrow surfaces and determine whether the viscoelastic properties have any effects on lubrication characteristics compared with their Newtonian counterparts. This perturbation scheme is used to derive coupled nonlinear partial differential equations governing the evolution of the fluid velocity and pressure in thin film flows. The leading-order problem corresponds to Newtonian lubrication solution [3, Chapter 3], [4, Chapter 6]. Numerical solution on the order of the Deborah number (*De*) yields corrections to the flow profiles due to viscoelasticity. Attention will be paid to the mechanisms of the viscoelastic pressure driving thin-film flow in the presence of viscoelasticity.

In Section 2, we present the governing equations with relevant scalings. In Section 3, we outline the perturbation method and provide analytical solutions for thin-film flows. In Section 4, we present a discussion of our numerical results. Finally, we present some concluding remarks in Section 5.

2. Mathematical model

One of the simplest viscoelastic fluid models available is the upper-convected Maxwell (UCM) model incorporating a constant viscosity and relaxation time. In this study, we restrict our attention to the UCM constitutive model characterized by a small relaxation time, λ. The continuity, momentum and constitutive equations for the incompressible flow of a non-Newtonian fluid are, respectively,

$$\nabla \cdot \mathbf{v} = 0, \tag{1}$$

$$\rho \left(\frac{\partial \mathbf{v}}{\partial t} + \mathbf{v} \cdot \nabla \mathbf{v} \right) = -(\nabla P + \nabla \cdot \boldsymbol{\tau}), \tag{2}$$

$$\lambda \overset{\nabla}{\boldsymbol{\tau}} + \boldsymbol{\tau} = -2\eta \mathbf{d},$$

where

$$\mathbf{d} = \frac{1}{2} \left(\nabla \mathbf{v} + (\nabla \mathbf{v})^T \right) \tag{4}$$

is the rate-of-deformation tensor, and $\overset{\nabla}{\boldsymbol{\tau}}$ is the upper-convected derivative defined as

$$\overset{\nabla}{\boldsymbol{\tau}} = \frac{\partial \boldsymbol{\tau}}{\partial t} + \mathbf{v} \cdot \nabla \boldsymbol{\tau} - (\nabla \mathbf{v}) \cdot \boldsymbol{\tau} - \boldsymbol{\tau} \cdot (\nabla \mathbf{v})^T. \tag{5}$$

In Equations (1–5), ρ is the constant lubricant density, $\mathbf{v} = (u, v)$ is the lubricant velocity vector, P is the pressure, $\boldsymbol{\tau}$, is the extra-stress tensor, λ. is the fluid relaxation time, and η is the lubricant viscosity. In general, λ and η are functions of the local shear rate, pressure and temperature (see, for example, [13, 18]). In this paper, they are taken to be constant.

A typical two-dimensional thin-film problem is illustrated in Figure 1, where the space between two surfaces in relative motion is filled with a non-Newtonian fluid. In this problem, we assume that the characteristic length L in the x-direction is much greater than the

characteristic length H_0 in the y-direction. Under the experimentally accessible processing conditions, the fluid may be assumed to incompressible and inertialess, and gravitational effects can be ignored. The continuity and momentum equations for steady flow can be rewritten in component form as

$$\frac{\partial u}{\partial x} + \frac{\partial v}{\partial y} = 0, \tag{6}$$

$$\frac{\partial \tau_{xx}}{\partial x} + \frac{\partial \tau_{xy}}{\partial y} + \frac{\partial P}{\partial x} = 0, \tag{7}$$

$$\frac{\partial \tau_{xy}}{\partial x} + \frac{\partial \tau_{yy}}{\partial y} + \frac{\partial P}{\partial y} = 0. \tag{8}$$

The constitutive equation (3) in component form reduces to

$$\tau_{xx} + \lambda \left(u\frac{\partial \tau_{xx}}{\partial x} + v\frac{\partial \tau_{xx}}{\partial y} - 2\frac{\partial u}{\partial y}\tau_{xy} - 2\frac{\partial u}{\partial x}\tau_{xx} \right) = -2\eta \frac{\partial u}{\partial x}, \tag{9}$$

$$\tau_{xy} + \lambda \left(u\frac{\partial \tau_{xy}}{\partial x} + v\frac{\partial \tau_{xy}}{\partial y} - \frac{\partial u}{\partial y}\tau_{yy} - \frac{\partial v}{\partial x}\tau_{xx} \right) = -\eta \left(\frac{\partial u}{\partial y} + \frac{\partial v}{\partial x} \right), \tag{10}$$

$$\tau_{yy} + \lambda \left(u\frac{\partial \tau_{yy}}{\partial x} + v\frac{\partial \tau_{yy}}{\partial y} - 2\frac{\partial v}{\partial y}\tau_{yy} - 2\frac{\partial v}{\partial x}\tau_{xy} \right) = -2\eta \frac{\partial v}{\partial y}. \tag{11}$$

With reference to Figure 1, the velocity boundary conditions are

$$u = U, \quad v = 0, \qquad \text{at} \quad y = 0, \tag{12}$$

$$u = 0, \quad v = 0, \qquad \text{at} \quad y = H(x), \tag{13}$$

where we assume that the lower surface is moving in the x-direct ion with velocity U. Equations (12–13) express the no-slip condition at both surfaces. The pressure boundary condition requires

$$P = P_a, \quad \text{at} \quad x = 0 \quad \text{and} \quad x = L. \tag{14}$$

Thus, the pressure at the ends of the gap reduces to that of a stationary fluid at ambient pressure P_a. In fact, there has been a long-standing controversy in the literature on lubrication as to the best end-pressure boundary conditions, as the choice of these conditions can significantly affect the prediction for a non-Newtonian model [4, p. 299], [9, Chapter 10], [13]. A discussion of the pressure boundary conditions at the inlet and the exit can be found in [3, pp.32–98], [4, Chapter 6], [9, Chapter 10], [19].

The governing equations can be expressed in dimensionless form in terms of the following dimensionless quantities

$$\begin{aligned}
&x^* = \frac{x}{L}, \quad y^* = \frac{y}{H_0}, \quad u^* = \frac{u}{U}, \quad v^* = \frac{v}{UH_0/L}, \\
&\tau_{xx}^* = \frac{\tau_{xx}}{\eta UL/H_0^2}, \quad \tau_{xy}^* = \frac{\tau_{xy}}{\eta U/H_0}, \quad \tau_{yy}^* = \frac{\tau_{yy}}{\eta U/L}, \\
&p = \frac{P - P_a}{\eta UL/H_0^2}, \quad itDe = \frac{\lambda U}{L}, \quad \epsilon = \left(\frac{H_0}{L}\right)^2, \quad h(x) = \frac{H(x)}{H_0}.
\end{aligned} \tag{15}$$

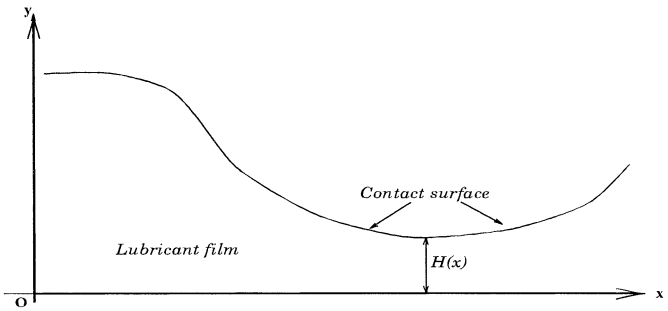

Figure 1. Geometry for a lubricant thin film flow.

The concept of the Deborah number highlights that it is not only the material's relaxation time, λ, which determines material behaviour, but also the time-scale of the deformation process. The Deborah number is zero for a Newtonian fluid and infinite for a Hookean elastic solid [4, p. 226], [8].

Substituting the dimensionless variables (15) in equations (6–11), and dropping the asterisks, we obtain the dimensionless governing equations

$$\frac{\partial u}{\partial x} + \frac{\partial v}{\partial y} = 0, \tag{16}$$

$$\frac{\partial \tau_{xx}}{\partial x} + \frac{\partial \tau_{xy}}{\partial y} + \frac{\partial p}{\partial x} = 0, \tag{17}$$

$$\epsilon \left(\frac{\partial \tau_{xy}}{\partial x} + \frac{\partial \tau_{yy}}{\partial y} \right) + \frac{\partial p}{\partial y} = 0, \tag{18}$$

$$\tau_{xx} + De \left(u \frac{\partial \tau_{xx}}{\partial x} + v \frac{\partial \tau_{xx}}{\partial y} - 2 \frac{\partial u}{\partial y} \tau_{xy} - 2 \frac{\partial u}{\partial x} \tau_{xx} \right) = -2\epsilon \frac{\partial u}{\partial x}, \tag{19}$$

$$\tau_{xy} + De \left(u \frac{\partial \tau_{xy}}{\partial x} + v \frac{\partial \tau_{xy}}{\partial y} - \frac{\partial u}{\partial y} \tau_{yy} - \frac{\partial v}{\partial x} \tau_{xx} \right) = - \left(\frac{\partial u}{\partial y} + \epsilon \frac{\partial v}{\partial y} \right), \tag{20}$$

$$\tau_{yy} + De \left(u \frac{\partial \tau_{yy}}{\partial x} + v \frac{\partial \tau_{yy}}{\partial y} - 2 \frac{\partial v}{\partial y} \tau_{yy} - 2 \frac{\partial v}{\partial x} \tau_{xy} \right) = -2 \frac{\partial v}{\partial y}, \tag{21}$$

and the boundary conditions

$$u = 1, \quad v = 0, \qquad \text{when} \quad y = 0, \tag{22}$$

$$u = 0, \quad v = 0, \qquad \text{when} \quad y = h(x), \tag{23}$$

$$p = 0, \qquad \text{when} \quad x = 0, \quad \text{and } x = 1. \tag{24}$$

In most cases, bubbles may appear in the convergent-divergent area, as shown in Figure 1, due to the pressure falling below the saturation level yielding a cavitation region. Since the governing equations are no longer valid in such a region, a cavitation model developed either by the form of variation inequality [19] or by introducing an additional unknown for the fluid

saturation pressure [13, 18] has to be considered. Details of the cavitation models can be found in [19], [20, pp. 207–228].

3. Theoretical analysis

In this section, we use a regular perturbation expansion to analyse Equations (16–21) subject to the boundary conditions (22–24). Specifically, we assume an asymptotic solution in the form of a double perturbation expansion in powers of ϵ and De:

$$\begin{aligned}
u &= u^{[\ell]} + \epsilon u^{[\epsilon]} + De u^{[D]} + O(\epsilon^2) + O(De^2),\\
v &= v^{[\ell]} + \epsilon v^{[\epsilon]} + De v^{[D]} + O(\epsilon^2) + O(De^2),\\
\tau_{xx} &= \tau_{xx}^{[\ell]} + \epsilon \tau_{xx}^{[\epsilon]} + De \tau_{xx}^{[D]} + O(\epsilon^2) + O(De^2),\\
\tau_{yy} &= \tau_{yy}^{[\ell]} + \epsilon \tau_{yy}^{[\epsilon]} + De \tau_{yy}^{[D]} + O(\epsilon^2) + O(De^2),\\
\tau_{xy} &= \tau_{xy}^{[\ell]} + \epsilon \tau_{xy}^{[\epsilon]} + De \tau_{xy}^{[D]} + O(\epsilon^2) + O(De^2),\\
p &= p^{[\ell]} + \epsilon p^{[\epsilon]} + De p^{[D]} + O(\epsilon^2) + O(De^2).
\end{aligned} \tag{25}$$

The leading term is the conventional lubrication solution denoted by the superscript $[\ell]$. The two perturbation corrections are denoted by the superscripts $[\epsilon]$ and $[De]$, respectively.

3.1. Zero-order solution

Substituting (25) in Equations 16–24), we obtain the following leading-order equations

$$\begin{aligned}
&\frac{\partial u^{[\ell]}}{\partial x} + \frac{\partial v^{[\ell]}}{\partial y} = 0,\\
&\tau_{xx}^{[\ell]} = 0, \qquad \tau_{yy}^{[\ell]} = -2\frac{\partial v^{[\ell]}}{\partial y},\\
&\tau_{xy}^{[\ell]} = -\frac{\partial u^{[\ell]}}{\partial y}, \quad \frac{\partial \tau_{xy}^{[\ell]}}{\partial y} + \frac{\partial p^{[\ell]}}{\partial y} = 0, \quad \frac{\partial p^{[\ell]}}{\partial y} = 0,\\
&u^{[\ell]} = 1, \quad v^{[\ell]} = 0, \quad \text{when} \quad y = 0,\\
&u^{[\ell]} = v^{[\ell]} = 0, \quad \text{when} \quad y = h(x),\\
&p^{[\ell]} = 0, \quad \text{when} \quad x = 0, 1.
\end{aligned} \tag{26}$$

These equations can be readily solved for the velocity and pressure, yielding

$$u^{[\ell]} = \frac{h^2}{2}\frac{\mathrm{d}p^{[\ell]}}{\mathrm{d}x}\left(\frac{y^2}{h^2} - \frac{y}{h}\right) + 1 - \frac{y}{h}, \tag{27}$$

$$v^{[\ell]} = \frac{\mathrm{d}h}{\mathrm{d}x}\left(2 - 3\frac{h_m}{h}\right)\left(\frac{y^3}{h^3} - \frac{y^2}{h^2}\right), \tag{28}$$

$$\frac{\mathrm{d}p^{[\ell]}}{\mathrm{d}x} = 6\frac{h - h_m}{h^3}, \tag{29}$$

where

$$h_m = \frac{\int_0^1 h^{-2}(x)\mathrm{d}x}{\int_0^1 h^{-3}(x)\mathrm{d}x}. \tag{30}$$

Integrating Equation (29), we obtain the pressure distribution

$$p^{[\ell]}(x) = 6\int_0^x h^{-2}(s)\mathrm{d}s - 6h_m \int_0^x h^{-3}(s)\mathrm{d}s, \tag{31}$$

which is a solution to the classical Reynolds equation [3, Chapter 3], [4, Chapter 6.2].

3.2. ϵ-ORDER EQUATIONS

The order-ϵ solution is now considered. We first substitute (25) in (16–24), and then collect all order-ϵ terms to obtain the governing equations

$$\frac{\partial u^{[\epsilon]}}{\partial x} + \frac{\partial v^{[\epsilon]}}{\partial y} = 0, \tag{32}$$

$$\tau_{xx}^{[\epsilon]} = -2\frac{\partial u^{\ell}}{\partial x}, \quad \tau_{xy}^{[\epsilon]} + \frac{\partial u^{[\epsilon]}}{\partial y} = -\frac{\partial v^{\ell}}{\partial y}, \quad \tau_{yy}^{[\ell]} = -2\frac{\partial v^{[\epsilon]}}{\partial y}, \tag{33}$$

$$\frac{\partial \tau_{xx}^{[\epsilon]}}{\partial x} + \frac{\partial \tau_{xy}^{[\epsilon]}}{\partial y} + \frac{\partial p^{[\epsilon]}}{\partial x} = 0, \tag{34}$$

$$\frac{\partial \tau_{xy}^{[\ell]}}{\partial x} + \frac{\partial \tau_{yy}^{[\ell]}}{\partial y} + \frac{\partial p^{[\ell]}}{\partial y} = 0, \tag{35}$$

with the boundary conditions

$$u^{[\epsilon]} = v^{[\epsilon]} = 0 \qquad \text{when } y = 0 \quad \text{and } y = h(x), \tag{36}$$

$$p^{[\epsilon]} = 0 \qquad \text{when } x = 0 \quad \text{and } x = 1. \tag{37}$$

Substituting $\tau_{xy}^{[\ell]}$, $\tau_{yy}^{[\epsilon]}$, $\tau_{xx}^{[\ell]}$ and $\tau_{xy}^{[\epsilon]}$ in Equations (34–35), we can simplify the above equations to

$$\frac{\partial p^{[\epsilon]}}{\partial x} = \frac{\partial^2 u^{[\epsilon]}}{\partial y^2} + 2\frac{\partial^2 u^{[\ell]}}{\partial x^2} + \frac{\partial^2 v^{[\ell]}}{\partial y^2}, \tag{38}$$

$$\frac{\partial p^{[\epsilon]}}{\partial y} = \frac{\partial^2 v^{[\ell]}}{\partial y^2}, \tag{39}$$

where $u^{[\ell]}$ and $v^{[\ell]}$ are given in (27) and (28).

3.3. De-ORDER EQUATIONS

Due to the small size of the ratio H_0/L, the ϵ terms in the stress governing equations (19–20) can be omitted. Under this approximation we substitute the expansion (25) in the governing equations (16–21), and collect terms of the same order *De* to obtain

$$\frac{\partial u^{[D]}}{\partial x}+\frac{\partial v^{[D]}}{\partial y}=0, \tag{40}$$

$$\tau_{xx}^{[D]}=2\frac{\partial u^{[\ell]}}{\partial y}\tau_{xy}^{[\ell]}=-2\left(\frac{\partial u^{[\ell]}}{\partial y}\right)^2, \tag{41}$$

$$\tau_{xy}^{[D]}+\frac{\partial u^{[D]}}{\partial y}=-u^{[\ell]}\frac{\partial \tau_{yy}^{[\ell]}}{\partial x}-v^{[\ell]}\frac{\partial \tau_{xy}^{[\ell]}}{\partial y}+\frac{\partial u^{[\ell]}}{\partial y}\tau_{yy}^{[\ell]}, \tag{42}$$

$$\tau_{yy}^{[D]}+2\frac{\partial v^{[D]}}{\partial y}=-u^{[\ell]}\frac{\partial \tau_{xy}^{[\ell]}}{\partial x}-v^{[\ell]}\frac{\partial \tau_{yy}^{[\ell]}}{\partial y}+2\frac{\partial v^{[\ell]}}{\partial y}\tau_{yy}^{[\ell]}+2\frac{\partial v^{[\ell]}}{\partial x}\tau_{xy}^{[\ell]}, \tag{43}$$

$$\frac{\partial \tau_{xx}^{[D]}}{\partial x}+\frac{\partial \tau_{xy}^{[D]}}{\partial y}+\frac{\partial p^{[D]}}{\partial x}=0, \tag{44}$$

$$\frac{\partial p^{[D]}}{\partial y}=0, \tag{45}$$

and the boundary conditions

$$u^{[D]}=v^{[D]}=0, \qquad \text{when} \quad y=0 \quad \text{and} \quad h=h(x), \tag{46}$$

$$p^{[D]}=0, \quad \text{when} \quad x=0,1. \tag{47}$$

Note that the equation $\tau_{xy}^{[\ell]}=-\frac{\partial u^{[\ell]}}{\partial y}$ has been used to simplify (41). Similar expressions can be found in [16].

Substituting $\tau_{xx}^{[D]}$ and $\tau_{xy}^{[D]}$ from Equations (41) and (42) in Equation (44), we obtain

$$\begin{aligned}-\frac{\partial^2 u^{[D]}}{\partial y^2}-2\frac{\partial}{\partial x}\left(\frac{\partial u^{[\ell]}}{\partial y}\right)^2-\frac{\partial}{\partial y}\left(u^{[\ell]}\frac{\partial \tau_{xy}^{[\ell]}}{\partial x}\right)-\frac{\partial}{\partial y}\left(v^{[\ell]}\frac{\partial \tau_{xy}^{[\ell]}}{\partial y}\right)\\ +\frac{\partial}{\partial y}\left(\tau_{yy}^{[\ell]}\frac{\partial u^{[\ell]}}{\partial y}\right)+\frac{\partial p^{[D]}}{\partial x}=0.\end{aligned} \tag{48}$$

From Equation (45), we know that the viscoelastic pressure $p^{[D]}$ is independent of y, hence, $\partial^2 u^{[D]}/\partial y^2$ in Equation (48) is also independent of y. We can integrate (48) twice with respect to y subject to the boundary conditions (46), and thus obtain a general expression for the perturbation velocity

$$u^{[D]}=\frac{h^2}{2}\frac{\mathrm{d}p^{[D]}}{\mathrm{d}x}\left(\frac{y^2}{h^2}-\frac{y}{h}\right)+\frac{1}{h}\frac{\mathrm{d}h}{\mathrm{d}x}\left(1-3\frac{h_m}{h}\right)\left(2-3\frac{h_m}{h}\right)\left(\frac{y^2}{h^2}-\frac{y}{h}\right). \tag{49}$$

It should be noted that $u^{[D]}$ is a quadratic function of y only, and the solution given by Tichy in [16] appears erroneous. A modified Reynolds equation can be derived from the continuity equation

$$\frac{1}{12}\frac{\mathrm{d}}{\mathrm{d}x}\left(h^3\frac{\mathrm{d}p^{[D]}}{\mathrm{d}x}\right)=\frac{\mathrm{d}^2h}{\mathrm{d}x^2}\left(-\frac{1}{3}+\frac{3}{2}\frac{h_m}{h}-\frac{3}{2}\frac{h_m^2}{h^2}\right)+\frac{1}{h}\left(\frac{\mathrm{d}h}{\mathrm{d}x}\right)^2\left(-\frac{3}{2}\frac{h_m}{h}+3\frac{h_m^2}{h^2}\right). \tag{50}$$

However, we must still find $p^{[D]}$. The best way to formulate an equation for $p^{[D]}$ is by integrating the velocity $u^{[D]}$ across the film from $y = 0$ to $y = h(x)$, to obtain the net flow rate at order *De*. In fact, we have not yet used the continuity equation. We do so in an integral form to derive another constraint on the velocity field, namely

$$h_d = \int_0^{h(x)} u^{[D]}(y)\mathrm{d}y. \tag{51}$$

The constant h_d is not known at this point. Equation (51) yields an equation for $\mathrm{d}p^{[D]}/\mathrm{d}x$ as a function of $h(x)$, $\mathrm{d}h/\mathrm{d}x$, h_m and h_d,

$$\frac{\mathrm{d}p^{[D]}}{\mathrm{d}x} = -18\frac{h_m^2}{h^5}\frac{\mathrm{d}h}{\mathrm{d}x} + 18\frac{h_m}{h^4}\frac{\mathrm{d}h}{\mathrm{d}x} - 4\frac{1}{h^3}\frac{\mathrm{d}h}{\mathrm{d}x} - 12\frac{h_d}{h^3}. \tag{52}$$

This is simply a first-order ordinary differential equation for the viscoelastic pressure gradient, which may be integrated to yield a solution, $p^{[D]}(x)$. Since this solution satisfies a first-order equation, a constant of integration appears. A second unknown constant h_d appears in Equation (52). Actually, these two constants can be uniquely defined if the boundary conditions (47) are imposed. Hence, we obtain an analytical solution for the pressure

$$p^{[D]}(x) = \frac{9}{2}\left(\frac{h_m^2}{h^4} - \frac{h_m^2}{h_0^4}\right) - 6\left(\frac{h_m}{h^3} - \frac{h_m}{h_0^3}\right) + 2\left(\frac{1}{h^2} - \frac{1}{h_0^2}\right) - 12h_d\int_0^x \frac{1}{h^3(s)}\mathrm{d}s, \tag{53}$$

where

$$h_d = \left\{\frac{3}{8}\left(\frac{h_m^2}{h_1^4} - \frac{h_m^2}{h_0^4}\right) - \frac{1}{2}\left(\frac{h_m}{h_1^3} - \frac{h_m}{h_0^3}\right) + \frac{1}{6}\left(\frac{1}{h_1^2} - \frac{1}{h_0^2}\right)\right\}\left(\int_0^1 \frac{1}{h^3(s)}\mathrm{d}s\right)^{-1}, \tag{54}$$

with h_0 and h_1 being the values of $h(x)$ at $x = 0$ and $x = 1$,respectively.

4. Numerical results and discussion

The asymptotic solution to the *exact* formulation of the UCM model given in (25) is the sum of the conventional lubrication solution, plus small corrections from the effects of the geometric parameter ϵ and the viscoelastic property of fluid (the Deborah number De). In this section, we only compute the corrections of the solution at order De for the pressure $p^{[D]}$. The velocity $u^{[D]}$ then can be calculated directly from Equation (49). In a practical sense, this is not restrictive because in the lubrication analysis the Deborah number *De* is always less than unity [8].

Inspection of the formulations of the pressure given in the previous section shows that the pressure gradient $\mathrm{d}p^{[\ell]}/\mathrm{d}x$ depends only on the function $h(x)$, while, the viscoelastic pressure gradient $\mathrm{d}p^{[D]}/\mathrm{d}x$ depends not only on the surface slope $\mathrm{d}h/\mathrm{d}x$, but also on the surface curvature $\mathrm{d}^2h/\mathrm{d}x^2$. To examine the influence of the film surfaces and the effect of the Deborah number, we investigate a viscoelastic thin film under the following contact dimensionless surface [16]

$$h(x) = 1 + ax + \frac{1}{2}b(x^2 - x), \tag{55}$$

where a is the average curve slope and b is the derivative of the curve slope (curvature). If b is positive, the surface is concave, otherwise, the surface is convex. In Figure 2, the surface slope

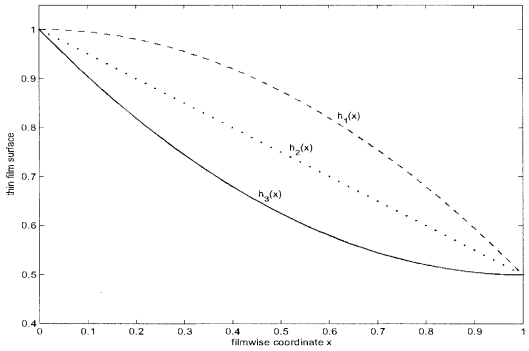

Figure 2. Profiles of three film surfaces: $h_1(x) = 1 - 0{\cdot}5x - 0{\cdot}5(x^2 - x)$, $h_2(x) = 1 - 0{\cdot}5x$ and $h_3(x) = 1 - 0{\cdot}5x + 0{\cdot}5(x^2 - x)$, respectively.

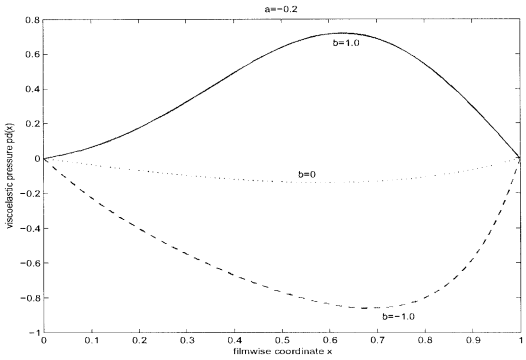

Figure 3. Plots of the viscoelastic pressure $p^{[D]}(x)$ for slope $a = -0{\cdot}2$ and curvatures $b = -1, b = 0$ and $b = 1$.

is $a = -0{\cdot}5$, and the curvatures are $b = -1$, $b = 0$ and $b = 1$, respectively. The minimum film thickness for these surfaces shown in Figure 2 is 0·5, and is attained at the fluid exit point $x = 1$. Other surfaces will be discussed in Section 4.2.

4.1. Effect of viscoelasticity on the pressure

In this section, we examine the effect of the Deborah number De on the solution of (53). For simplicity, the dimensionless film surface (55) is used with surface slopes $a = -0{\cdot}2$, $a = -0{\cdot}5$ and $a = -0{\cdot}8$, and curvatures $b = -1{\cdot}0$, $b = 0$ and $b = 1{\cdot}0$, respectively.

First, we examine the effect of a small value of the surface slope $a = -0{\cdot}2$ with curvatures $b = -1$, $b = 0$ and $b = 1$, respectively. Figure 3 shows plots of the viscoelastic pressures for these parameter values. It is found that for a small surface slope $a = -0{\cdot}2$ the viscoelastic pressures are negative when $b = -1$ and $b = 0$, and the maximal pressures, $|p^{[D]}(x)|$, are attained near the middle of the film. However, for the same surface slope, the viscoelastic pressure becomes positive when $b = 1$, and the maximal pressure is attained near the middle of the film. Clearly, the positions of these three maximum pressures are not coincident, or with the minimum film thickness point, which is $x = 1{\cdot}0$ in this example.

Next, we examine the effect of the mean value of the surface slope $a = -0{\cdot}5$ with different curvatures. The results are illustrated in Figure 4, where the viscoelastic pressures $p^{[D]}(x)$ are plotted with the curvature parameters $b = -1, b = 0$ and $b = 1$, respectively. As expected, the viscoelastic pressures are negative when $b = -1$ and $b = 0$. However, when $b = 1$, the viscoelastic pressure can be negative or positive, as shown in Figure 4. This feature is not seen when the surface slope is small. Furthermore, it is found that the maximum viscoelastic pressures, $|p^{[D]}(x)|$, are attained away from the middle of the film and approach the fluid exit point, compared with the case of small surface slope, as shown in Figure 3.

Finally, we consider the effect of a large surface slope $a = -0{\cdot}8$ with different curvatures. Figure 5 displays a comparison of the viscoelastic pressures for three different curvatures $b = -1, b = 0$ and $b = 1$. It is interesting that these three pressures are all negative. When the curvature changes from $b = 1$ to $b = -1$, the absolute value of the viscoelastic pressure increases. This means that the viscoelastic effect on the pressure is much stronger when the average surface slope is bigger. The positions of the maximum pressures $|p^{[D]}(x)|$ are very

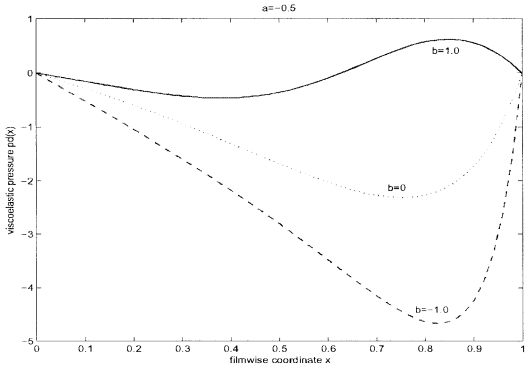

Figure 4. Plots of the viscoelastic pressure $p^{[D]}$ for slope $a = -0{\cdot}5$ and curvatures $b = -1$, $b = 0$ and $b = 1$.

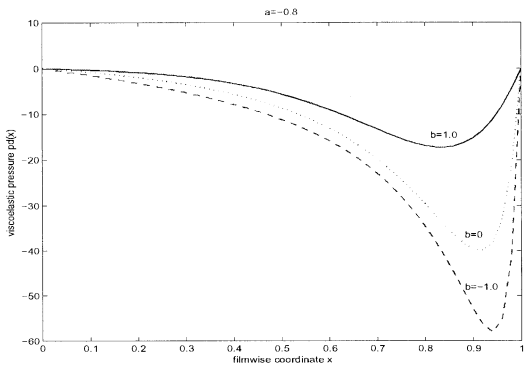

Figure 5. Plots of the viscoelastic pressure $p^{[D]}$ for slope $a = -0{\cdot}8$ and curvatures $b = -1, b = 0$ and $b = 1$.

close to the fluid exit point. If we look more carefully at the sequences of Figures 3–5, we find that the absolute values of the viscoelastic pressure increase with increasing surface slope parameters. For example, given a curvature, say $b = -1$, the maximum pressure $|p^{[D]}(x)|$ is about 0·85 when the slope is $a = -0{\cdot}8$, and about 4·5 when $a = -0{\cdot}5$, However, when the surface slope is $a = -0{\cdot}8$, the maximum pressure is dramatically increased over 55. Moreover, the positions of the maximum pressure move gradually from near the middle of the film to the minimum film thickness point, We suspect that this occurs for the following reason. When fluid enters the gap, material elements become more extended, As a consequence of this, and the viscoelasticity of the fluid, the first normal stress difference increases when the minimum film thickness point is approached. Thus, there will be a gradient in the first normal stress difference: which is highest near the minimum film thickness point and decreases upstream. These higher tensions near the point of the minimum film thickness will tend to pull fluid toward the minimum point. Because more fluid will enter the gap, the maximum pressure may increase to turn back same of the additional fluid.

In general, the viscoelastic pressure may either increase or decrease depending on combinations of the surface slope and its curvature. The larger the surface slope, the stronger the effect of the viscoelastic pressure. Numerical results obtained in this section demonstrate that viscoelasticity plays an important role in determining the pressure distributions, and it should be taken into account in the analysis of thin film flows.

4.2. Effect of the minimum film thickness

As discussed in the previous section, the influence of the film-surface shape is of considerable importance in the thin-film flow analysis. In order to further examine this effect on the pressure distribution, we consider three different film surfaces in this section: $h_1(x) = 0{\cdot}8 - 0{\cdot}5x + (x^2 - x)$, $h_2(x) = 0{\cdot}67 - 0{\cdot}5x + (x^2 - x)$, and $h_3(x) = 0{\cdot}64 - 0{\cdot}5x + (x^2 - x)$, plotted in Figure 6. Unlike the surfaces shown in Figure 2, these surfaces have the same average slope and curvature parameters, but, different minimum film thicknesses attained at the same point $x = 0{\cdot}75$, as shown in Figure 6. In these three surfaces, the minimum film thicknesses are $h_1^{\min} = 0{\cdot}2376$, $h_2^{\min} = 0{\cdot}1076$, and $h_3^{\min} = 0{\cdot}0776$, respectively. A comparison of the viscoelastic pressures corresponding to these three surfaces is illustrated

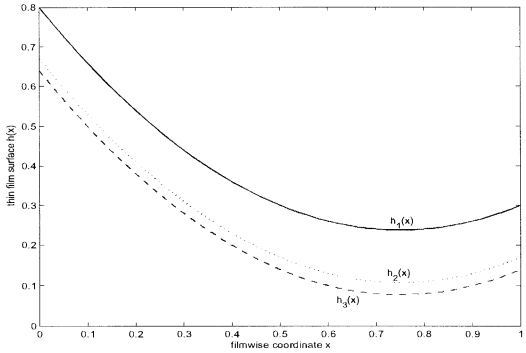

Figure 6. Profiles of the surfaces described by $h_1(x) = 0{\cdot}8 - 0{\cdot}5x + (x^2 - x)$, $h_2(x) = 0{\cdot}67 - 0{\cdot}5x + (x^2 - x)$, and $h_3(x) = 0{\cdot}64 - 0{\cdot}5x(x^2 - x)$.

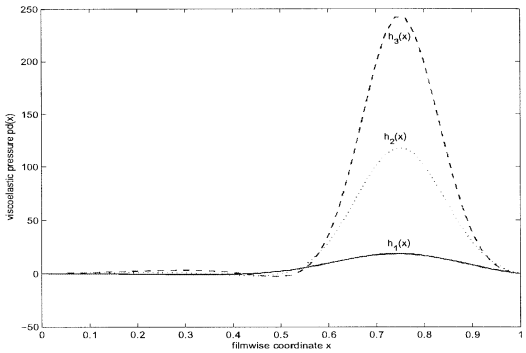

Figure 7. Comparison of the viscoelastic pressures corresponding to the three different surfaces $h_1(x)$, $h_2(x)$ and $h_3(x)$ given in Figure 6.

in Figure 7, where it can be seen that all maximum pressures are located almost at the same point, $x = 0{\cdot}75$, which is the position of the minimum film thickness for all three cases. More important, we also found that the magnitude of the viscoelastic pressure , increases dramatically with decreasing the minimum film thickness. Indeed, we find that, when the minimum film thickness is $h_1^{\min} = 0{\cdot}2376$, the maximum pressure is 18 for the surface $h_1(x)$; when the film thickness is $h_2^{\min} = 0{\cdot}1076$, the maximum pressure gradually increases to $h_3^{\min} = 0{\cdot}0776$. Moreover, when the film thickness decreases to $h_3^{\min} = 0{\cdot}0776$, the maximum pressure rapidly increases to 242. This behavior clearly suggests that there is a significant pressure enhancement when the minimum film thickness becomes small. Such a phenomenon is not observed in Newtonian fluids. It is worth pointing out that this viscoelastic pressure enhancement has been observed in experimental measurements for a journal bearing system [6], where it was found that viscoelasticity does indeed produce a measurable effect on lubrication characteristics at the higher eccentricity ratios (equivalent to a smaller minimum film thicknesses). Thus, we observe that our numerical predictions are in good agreement with the experimental observations in regard to the viscoelastic pressure enhancement in the thin film flows.

5. Conclusions

In this paper, we have readdressed the question as to whether the viscoelastic properties of a non-Newtonian fluid can have an effect on lubrication characteristics in thin-film flows. A perturbation analysis based on the upper-convected Maxwell constitutive equation was presented by employing the characteristic lubricant relaxation time in an order-of-magnitude analysis. Despite inherent limitations of the perturbation method, the approach presented here demonstrates a reasonable way to determine the viscoelastic effects on the lubricant characteristics in thin-film flows. The calculations in this paper are based on a UCM fluid model with constant viscosity and relaxation time. Numerical results show that the viscoelastic pressure depends on combinations of the surface slope and its curvature. When the surface slope is small, the effect of the viscoelastic pressure is small and hence can be ignored. However, when the surface slope is large, the influence of the viscoelastic pressure can be strong. Hence, it should be carefully taken into account in the analysis of thin-film flows. Furthermore, we

have found that the effect of viscoelasticity on the pressure is dominated by the minimum film thicknesses. Numerical simulations indicate that there is a significant enhancement of the viscoelastic pressure when the minimum film thickness is sufficiently small. This mechanism is associated with a beneficial effect of viscoelasticity on lubrication characteristics as observed in experimental measurements [6]. In conclusion, we have addressed and assessed some of the issues concerning viscoelastic effects on lubricant thin-film flows, although further work is needed to extend this method to other fluid-flow configurations.

Acknowledgements

The authors gratefully acknowledge the referees for their valuable comments on improving the presentation of the paper, and one referee, in particular, for proposing the analytical solution (53).

References

1. H. A. Barnes, J. F. Hutton and K. Walters, *An Introduction to Rheology*. Amsterdam: Elsevier (1989) 212pp.
2. R. B. Bird, R. C. Armstrong and O. Hassager, *Dynamics of Polymetric Liquids, Vol. 1, Fluid Mechanics.* New York: John Wiley and Sons (1987) 672pp.
3. A. Cameron, *Basic Lubrication Theory*. London: Longman Group Limited (1971) 195pp.
4. R. I. Tanner, *Engineering Rheology*. Second Edition, Oxford: Oxford University Press (2000) 559pp.
5. M. J. Davies and K. Walters, The behaviour of non-newtonian lubricants in Journal bearings – a theoretical study. In: T. C. Davenport (ed.), *Rheology of Lubricants*. New York: Applied Science Publishers (1972) pp. 16–37.
6. B. P. Williamson, K. Walters, T. W. Bates, R. C. Coy and A. L. Milton, The viscoelastic properties of multigrade oils and their effect on journal-bearing characteristics. *J. Non-Newtonian Fluid Mech.* 73 (1997) 115–126.
7. T. W. Bates, B. Williamson, J. A. Spearot and C. K. Murphy, A correlation between engine oil rheology and oil film thickness in engine journal bearing. *Soc. Automotive Eng.* Paper No. 860376, (1986).
8. M. J. Crochet and K. Walters, Computational rheology: a new science. *Endeavour, New Series* 17 (1993) 64–77.
9. A. Z. Szeri, *Fluid Film Lubrication Theory and Design*. Cambridge: Cambridge University Press (1998) 414pp.
10. G. W. Roberts and K. Walters, Oil viscoelastic effects in journal bearing lubrication. *Rheol Acta* 31 (1992) 55–62.
11. A. Rastogi and R. K. Gupta, Lubricant elasticity and the performance of dynamically loaded journal bearings. *J. Rheol.* 34 (1990) 1337–1356.
12. A. Z. Szeri, Some extensions of the lubrication theory of Osborne Reynolds. *ASME J. Tribology* 109 (1987) 21–37.
13. A. R. Davies and X. K. Li, Numerical modelling of pressure and temperature effects in viscoelastic flow between eccentrically rotating cylinders. *J. Non-Newtonian Fluid Mech.* 54 (1994) 331–350.
14. D. Dowson and G. R. Higginson, *Elastic-hydrodynamic Lubrication*. New York: Pergamon Press (1977) 235pp.
15. E. R. Khayat, Transient two-dimensional coating flow of a viscoelastic fluid on a substracte of arbitrary shape. *J. Non-Newtonian Fluid Mech.* 95 (2000) 199–233.
16. J. A. Tichy, Non-Newtonian lubrication with the convected Maxwell model. *Transactions of the ASME*. 118 (1996) 344–348.
17. Y. L. Zhang, O. K. Matar and R. V. Craster, Surfactant spreading on a thin weakly viscoelastic film. *J. Non-Newtonian Fluid Mech.* 105 (2002) 53–78.
18. X. K. Li, D. Gwynllyw, A. R. Davies and T. N. Phillips, Three-dimensional effects in dynamically loaded journal bearings. *Int. J. Nurner. Methods Fluids* 29 (1999) 311–341.
19. D. Dowson and C. M. Taylor, Cavitation in bearings. *Annu. Rev. Fluid Mech.* 11 (1979) 35–66.
20. C. E. Brennen, *Cavitation and Bubble Dynamics*. Oxford: Oxford University Press (1995) 282 pp.